

Chemical Abundances of M giants in the Galactic Center: a Single Metal-Rich Population with Low $[\alpha/\text{Fe}]^*$

N. Ryde¹ and M. Schultheis²

¹ Department of Astronomy and Theoretical Physics, Lund Observatory, Lund University, Box 43, 221 00, Lund, Sweden e-mail: ryde@astro.lu.se

² Observatoire de la Côte d’Azur, CNRS UMR 7293, BP4229, Laboratoire Lagrange, 06304 Nice Cedex 4, France e-mail: mathias.schultheis@oca.eu

Submitted 2013; accepted 2014

ABSTRACT

Context. The formation and evolution of the Milky Way bulge is still largely an unanswered question. One of the most essential observables needed in its modelling are the metallicity distribution and the trends of the α elements as measured in stars. While Bulge regions beyond $R \gtrsim 50$ pc of the centre has been targeted in several surveys, the central part has escaped detailed study due to the extreme extinction and crowding. The abundance gradients from the center are, however, of large diagnostic value.

Aims. We aim at investigating the Galactic Centre environment by probing M giants in the field, avoiding supergiants and cluster members.

Methods. For 9 field M-giants in the Galactic Centre region, we have obtained high- and low-resolution spectra observed simultaneously with CRIRES and ISAAC on UT1 and UT3 of the VLT. The low-resolution spectra provide a means of determining the effective temperatures, and the high-resolution spectra provide detailed abundances of Fe, Mg, Si, and Ca.

Results. We find a metal-rich population at $[\text{Fe}/\text{H}] = +0.11 \pm 0.15$ and a lack of the metal-poor population, found further out in the Bulge, corroborating earlier studies. Our $[\alpha/\text{Fe}]$ element trends, however, show low values, following the outer Bulge trends. A possible exception of the $[\text{Ca}/\text{Fe}]$ trend is found and needs further investigation.

Conclusions. The results of the analysed field M-giants in the Galactic Centre region, excludes a scenario with rapid formation, in which SNIe played a dominated role in the chemical enrichment of the gas. The metal-rich metallicities together with low α -enhancement seems to indicate a bar-like population perhaps related to the nuclear bar.

Key words. Galaxy: bulge, structure, stellar content – stars: fundamental parameters: abundances -infrared: stars

1. Introduction

The formation of the Milky Way bulge remains a puzzle. Abundance ratios of key elements as measured in bulge stars of different populations and at different locations, can set empirical constraints on the formation and evolution of the Bulge (see e.g. Silk & Wyse 1993; Matteucci 2012). While more and more detailed¹ elemental abundance determinations of stars in the intermediate and outer Bulge (such as Baade’s window) have emerged, the study of detailed abundances in Bulge regions within projected distances of $R \lesssim 50$ pc of the Galactic Centre has until recently been prevented due to regions of high extinction (see e.g. Schultheis et al. 2009) and the lack of sensitive high-resolution IR spectrographs. Extinction of 10-30 magnitudes in the V band can, however, be overcome by investigating stars in the K band, where the extinction is a factor of 10 lower (Cardelli et al. 1989).

The abundance gradient with latitude is an important diagnostic of the properties and formation history of the Bulge (Grieco et al. 2012). While the outer bulge shows evidence for a metallicity gradient (see e.g. Hill et al. 2011), be it due to a true gradient in a population or the relative change in proportions

of two or more populations, only a few studies have investigated abundance gradients in the inner bulge. Rich et al. (2007) studied detailed abundances of M-giants in a field at $(l, b) = (0^\circ, -1^\circ)$, while Rich et al. (2012) studied fields located at lower latitudes: $(l, b) = (0^\circ, -1.75^\circ)$ and $(l, b) = (1^\circ, -2.65^\circ)$. They find an iron abundances of $[\text{Fe}/\text{H}] = -0.2 \pm 0.1$ for all three fields, indicating a lack of any major vertical abundance-gradient. A detailed abundance study in the Galactic Center (GC) region itself is missing. Until now, most of the chemical abundance studies were limited to luminous supergiants making the abundance analysis difficult due to their complex and extended stellar atmospheres. Carr et al. (2000), Ramírez et al. (2000), and Davies et al. (2009) analysed high-resolution spectra of supergiant stars in the GC region, indicating metallicities of nearly solar metallicity. A similar conclusion was obtained by Najarro et al. (2009) analysing two luminous blue variables. Cunha et al. (2007) derived abundances of a few M giants in the Central Cluster and found a metallicity of $[\text{Fe}/\text{H}] = +0.14 \pm 0.06$, together with enhanced $[\text{O}/\text{Fe}]$ and $[\text{Ca}/\text{Fe}]$ abundances of +0.2 and +0.3, respectively, indicating that SN II played a dominant role in the chemical enrichment of the gas for this cluster.

Here, we present an analysis, based on near-IR, high-resolution spectra, of 9 M-giant stars located in the GC, only 2.5 – 5.5 arcminutes North of the very center of the Milky Way, which corresponds to a projected galactocentric distance of 5 – 10 pc. Our goal is to obtain the metallicity distribution

* Based on observations collected at the European Southern Observatory, Chile, program number 089.B-0312(A)/VM/CRIRES and 089.B-0312(B)/VM/ISAAC

¹ at spectral resolutions of $R = \lambda/\Delta\lambda \gtrsim 50000$

Table 1. Basic data for the observed stars and their stellar parameters.

Star	RA (J2000) (h:m:s)	Dec (J2000) (d:am:as)	K^a	K_0	exp. time [s]	T_{eff} [K]	$\log g$ (cgs)	[Fe/H]	ξ_{macro} km s^{-1}	v_{rad} km s^{-1}	SNR pixel^{-1}
Galactic centre stars											
GC1	17:45:35.43	-28:57:19.28	11.90	9.40	3000	3668	1.37	+0.19	6.6	+45.2	55
GC20	17:45:34.95	-28:55:20.17	11.68	9.37	3600	3683	0.76	+0.18	8.1	-8.4	50
GC22	17:45:42.41	-28:55:52.99	11.54	9.04	3600	3618	0.70	+0.02	6.0	-123.5	90
GC25	17:45:36.34	-28:54:50.41	11.60	9.10	2400	3340	0.77	+0.08	7.6	-9.7	50
GC27	17:45:36.72	-28:54:52.37	11.64	9.14	3600	3404	1.16	+0.31	8.1	-210.8	50
GC28	17:45:38.13	-28:54:58.32	11.67	9.17	3000	3773	1.24	-0.13	5.7	+145.0	50
GC29	17:45:43.12	-28:55:37.10	11.59	9.09	3600	3420	0.74	+0.10	8.0	-304.9	70
GC37	17:45:35.94	-28:58:01.43	11.50	9.00	3600	3754	0.93	-0.04	7.7	-104.0	70
GC44	17:45:35.95	-28:57:41.52	11.58	9.24	3600	3465	0.83	+0.29	6.9	-136.3	70
Disk stars											
α Boo ^b	14:15:39.67	+19:10:56.7	-2.91		atlas	4286	1.66	-0.52	6.3	+26.5	250
BD-012971	14:38:48.04	-02:17:11.5	4.30		16	3573	0.50	-0.78	9.3	+21.5	150
142173 ^c	00:32:12.56	-38:34:02.3	9.29		240	4330	1.50	-0.77	9.3	-86.0	130
171877 ^c	00:39:20.23	-31:31:35.5	8.12		240	3975	1.10	-0.93	7.0	-30.5	150
225245 ^c	00:54:46.38	-27:35:30.4	8.79		240	4031	0.65	-1.16	6.6	-48.3	130
313132 ^c	01:20:20.66	-34:09:54.1	7.04		120	4530	2.00	-0.20	8.7	-54.4	190
343555 ^c	01:29:42.01	-30:15:46.4	8.46		240	4530	2.25	-0.74	6.8	-161.7	240
HD 787	00:12:09.99	-17:56:17.8	1.86		4	4020	0.85	-0.16	8.2	-39.7	110

Notes. ^a K magnitude of the GC stars from Nishiyama (private comm.) and of the disk stars from 2MASS.

^b The fundamental parameters of α Boo are taken from Ramírez & Allende Prieto (2011).

^c Identification number from the Southern Proper-Motion Program (SPM III Girard et al. 2004), as given in Monaco et al. (2011).

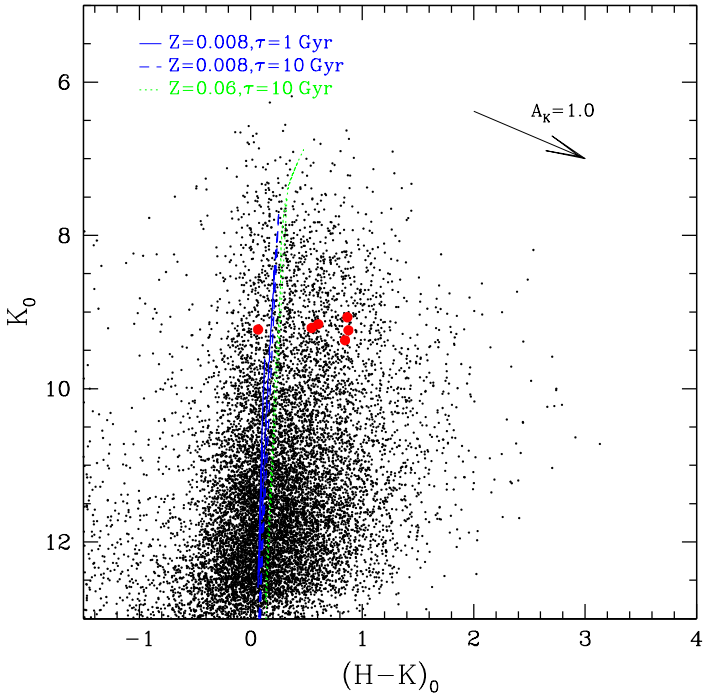


Fig. 1. Dereddened $(H - K)_0$ vs. K_0 diagram of the GC field using the data of Nishiyama et al. and the extinction map of Schultheis et al. (2009). In red are indicated our selected M giants. The blue lines show the Padova isochrones with $Z=0.008$ and $\tau = 1$ Gyr (solid line) and $\tau = 10$ Gyr (dashed line) while the green line at $Z=0.06$ and $\tau = 10$ Gyr. The arrow on the top right shows the extinction vector of $A_K = 1$ mag (Nishiyama et al. 2009).

and the corresponding α -element abundances (Mg, Si, Ca) of GC stars.

2. Observations

When selecting our GC stars, we used the Nishiyama et al. (2009) dataset and dereddened our sources using the extinction map of Schultheis et al. (2009). Due to the high extinction, we selected field red giants (avoiding cluster and supergiant stars) based on the dereddened $(H - K)_0$ vs. K_0 diagram covering the full $(H - K)_0$ colour range to avoid any selection bias. Figure 1 shows the dereddened CMD together with our selected M giants superimposed by the Padova isochrones with $Z=0.008$ and $Z=0.06$ and ages of 1 Gyr and 10 Gyr. Unfortunately the $H-K$ colour is very insensitive to the age of population making it impossible to constrain the age and therefore the mass of our stars. In addition, to ensure that our sources are located in the GC itself, we used the high-resolution, 3D interstellar-extinction maps of the galactic Bulge of Schultheis et al. (2014), who used the VVV data set in distance bins of 500 pc. We placed our stars on these 3D extinction plots and found that our stars lie between 7–9 kpc which rules out any possible foreground contamination. We are therefore confident that all our ‘Bulge’ stars, presented in Table 1, belong to the GC. The six local thick-disk stars, the thin-disk star BD-012971, and the reference star α Boo, which we also analyse in the same way as for the GC stars, are also given in Table 1.

On 27–29 June 2012, we observed the M giants close to the Galactic Centre and the disk stars given in Table 1 in the near-infrared with the *Very Large Telescope*, VLT. Every star was observed both using the low-resolution spectrometer ISAAC (Moorwood et al. 1998) and the high-resolution spectrometer CRIRES (Käufl et al. 2004), mounted on UT3 and UT1, respectively, of the VLT. The ISAAC spectrometer, with a spectral resolution of $R \sim 1000$ and a wavelength range between 2.00–2.53 μm , was used to determine the effective temperature of our stars, for details see Schultheis & Ryde, in prep. CRIRES uses, following standard procedures (Smoker 2007),

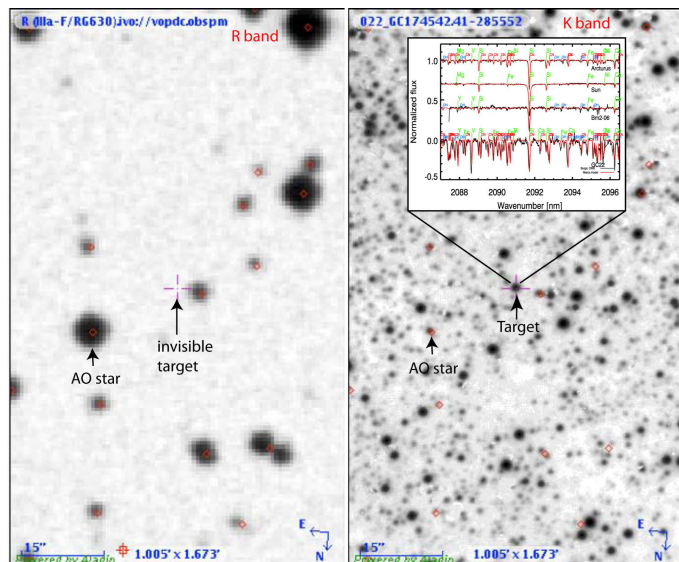


Fig. 2. An example of a finding chart from our observing run with CRIRES at the VLT. The target star, GC22, shown here, is one of our 9 M giants in the Galactic Centre field, with stars only 2.5 – 5.5' North of the very center of the Milky Way. The left panel is an image in the R band at 660 nm (from the VO-Paris Data Centre in Paris, observed with the ESO Schmidt telescope), while the right one shows the very same field but at 2.2 μ m (a UKIDSS K-band image from DR9, see Lawrence et al. 2013). The large difference in appearance is caused by the massive dust extinction towards this field, prohibiting optical spectroscopy. The inset shows our K band spectrum of GC22, from which we can derive the Fe, Mg, Si, and Ca abundances. The *Adaptive Optics* (AO) system works in the R band.

nodding on the slit and jittering to reduce the sky background and the Adaptive Optics (AO) MACAO system to enhance the amount of light captured by the slit. Due to the large crowding in our field (see Figure 2), special care had to be taken of the orientation of the 40'' long slit. For the CRIRES observations, we used a 0.''4 wide slit ($R \sim 50000$), and a standard setting ($\lambda_{\text{vac}}^{\text{ref}} = 2105.5$, order=27) with an unvignetted spectral range covering 20818 – 21444 Å, with three gaps (20 Å) between the four detector arrays. We aimed at a signal-to-noise ratio per pixel of 50-100 depending on the brightness of the stars. When selecting our stars, an instrumental constraint was set by the requirements that the wavefront sensing is done in the R band. For optimal AO performance, the guide star has preferably to be brighter than $R = 14$ and within 15'' of the science object. The reductions of the CRIRES observations were done by following standard recipes (Smoker et al. 2012) using Gasgano (Klein Gebbinck et al. 2007). Subsequently, we used IRAF (Tody 1993) to normalise the continuum, eliminate obvious cosmic hits, and correct for telluric lines (with telluric standard stars). Two examples of CRIRES spectra are shown in Figure 3.

3. Analysis

The derived stellar parameters of our stars are given in Table 1. Ramirez et al. (1997), Ivanov et al. (2004), and Blum et al. (2003) studied the behaviour of the ^{12}CO band-head situated at 2.3 μ m with low-resolution K-band spectra and found a remarkably tight relation between the equivalent width and the effective temperature for M giants. We therefore analysed our ISAAC spectra guided by their work. The analysis of our observations of

additional calibration stars with known effective temperatures, leads to a tight relation between T_{eff} and the CO band intensity for $3200 < T_{\text{eff}} < 4000$ (Schultheis & Ryde in prep.). The typical r.m.s error is in the order of 100 K. We were able to apply this method for all but three of our stars; For the three warmer thick-disk stars, which have temperatures beyond the bound of our temperature calibration (the reason being that the CO-band strength weakens and is virtually unmeasurable), we had to resort to the temperature determination of Monaco et al. (2011), which also was the source of our thick disk stars. These authors determined the effective temperatures by imposing a common Fe abundance from Fe I lines of different excitation energies.

The surface gravities of our GC stars were determined in a similar way as Zoccali et al. (2008) by adopting a mean distance of 8 kpc to the GC, $T_{\odot} = 5770$ K, $\log g_{\odot} = 4.44$, $M_{\text{bol},\odot} = 4.75$ and $M_{\star} = 1.0 M_{\odot}$. H and Ks band photometry from the VVV survey (Minniti et al. 2010), extinction values from Schultheis et al. (2009), and the bolometric corrections from Houdashelt et al. (2000) have been used. The surface gravity of all our disk stars are taken from the Monaco et al. (2011) determination, except the thin disk star BD-012971, whose surface gravity was taken from Rich & Origlia (2005).

Our CRIRES spectra were analysed using the software *Spectroscopy Made Easy*, *SME* (Valenti & Piskunov 1996, 2012) with a grid of MARCS spherical-symmetric, LTE model-atmospheres (Gustafsson et al. 2008). SME is a spectral synthesis program that uses a grid of model atmospheres in which it interpolates for a given set of fundamental parameters. The program then derives an abundance from an observed spectral line by iteratively synthesising spectra which are compared to the observations by calculating the χ^2 . The program then finds the best fit, with the abundance as a free parameter, by minimising the χ^2 . For details, see Valenti & Piskunov (1996).

An atomic line-list based on an extraction from the VALD database (Piskunov et al. 1995) is used. Due to inaccurate atomic data, atomic lines were fitted to the solar intensity spectrum of Livingston & Wallace (1991), by our determining astrophysical $\log gf$ values for, most importantly, Fe, and Si lines. The metallicity and Si abundance we thus derive for α Boo are within 0.05 dex of the values determined by Ramírez & Allende Prieto (2011). However, since the Ca lines are very weak in the solar spectrum and the Mg lines are impossible to fit, we have determined their line strengths such that they fit the Arcturus flux spectrum of Hinkle et al. (1995) instead, with a Mg and Ca abundance from Ramírez & Allende Prieto (2011); $[\text{Mg}/\text{Fe}] = 0.37$ and $[\text{Ca}/\text{Fe}] = 0.11$. In the syntheses we have also included a line list of the only molecule affecting this wavelength range, namely CN (Jørgensen & Larsson, 1990).

The microturbulence, χ_{micro} , is difficult to determine empirically, but is nevertheless important for the spectral syntheses, affecting saturated lines. We have chosen to use a typical value found in detailed investigations of red giant spectra in the near-IR by Tsuji (2008). The microturbulence is more than a km s^{-1} larger when determined from near-IR spectra compared to optical ones. We have therefore chosen a generic value of $\chi_{\text{micro}} = 2.0 \text{ km s}^{-1}$, see also the discussion in Cunha et al. (2007). Furthermore, in order to match our synthetic spectra with the observed ones, we also convolve the synthetic spectra with a 'macroturbulent' broadening, χ_{macro} , which takes into account the macroturbulence of the stellar atmosphere and instrumental broadening. These were determined by matching the prominent Si line at 20917.1 Å and the two Al lines at 21093.08 Å and 21163.82 Å.

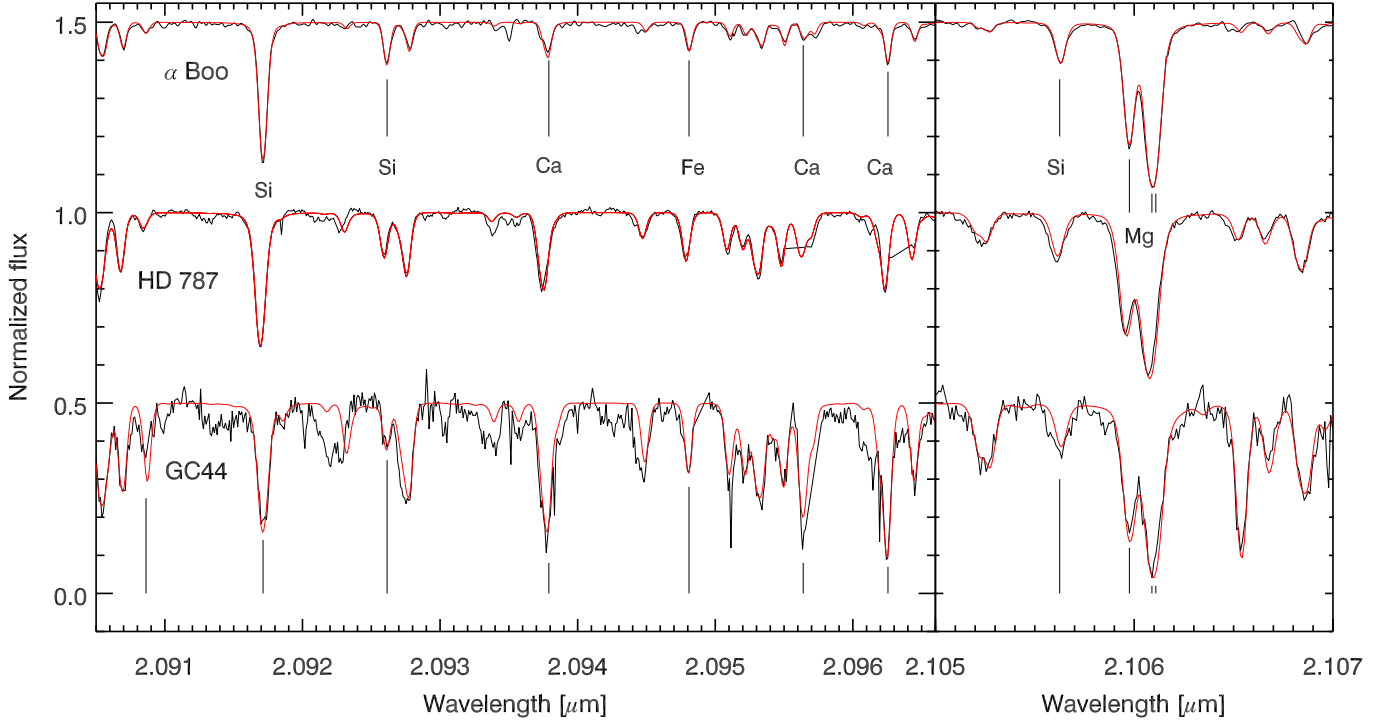


Fig. 3. Spectra of wavelength regions covering a few of the lines used for the abundance determination. Other features not marked are mostly due to CN. The top spectrum is from the Arcturus atlas (Hinkle et al. 1995), the middle one is of the thick disk star HD 787, and the bottom spectrum is of the Galactic Centre star GC44. The flat regions of the HD 787 spectrum at 2.0955 and 2.0963 μm are due to the elimination of cosmic hits.

The iron (giving the metallicity), Mg, Si, and Ca abundances were then determined by χ^2 minimisation between the observed and synthetic spectra for, depending on star, 6 – 9 Fe, 2 – 6 Si, 1 – 4 Ca, 2 Mg, and typically 10 CN lines. These abundances are presented in Table 2 and the synthesised spectra are shown with the observed ones for a few typical stars in Figure 3 and for all our spectra in the online only Figures 8 and 9.

The uncertainties in the determination of the abundance ratios, for typical uncertainties in the stellar parameters are all modest, within 0.1 dex (see Schultheis & Ryde, in prep.), see also Table 3. Note, specifically the relatively small uncertainty in the abundance ratio due to a variation of the microturbulence parameter, ξ_{micro} . This demonstrates that the lines are not badly saturated, and therefore they should be sensitive to the abundances. In Figure 4 the sensitivity of the spectral lines to a change of 0.2 dex in abundance is shown. The lines are obviously useful for an abundance determination for these stars.

4. Results and Discussion

Figure 5 shows the abundance ratio trends for Mg, Si, and Ca as derived from our GC stars in red and our local thick-disk stars in blue. In black we show the micro-lensed bulge dwarfs from the outer bulge ($|b| > -2^\circ$) as determined by Bensby et al. (2013). Within uncertainties, our thick disk trend as well as the Mg and Si trends follow the outer bulge trends, with low values of $[\alpha/\text{Fe}]$ at $[\text{Fe}/\text{H}] > -0.2$, although the GC stars show a much more narrow spread in $[\text{Fe}/\text{H}]$. Our $[\text{Ca}/\text{Fe}]$ in the GC show a higher trend than the outer bulge stars, actually in agreement with Cunha et al. (2007) and one of the outer bulge stars. With random uncertainties being of the order of 0.1 dex, this trend is significantly higher. This difference between Mg, Si, and Ca is not expected theoretically (Matteucci, private comm.), and sys-

Table 2. Derived abundances

Star	[Fe/H]	[Mg/Fe]	[Si/Fe]	[Ca/Fe]
GC1	0.19	0.11	0.12	0.16
GC20	0.18	0.10	0.10	0.21
GC22	0.02	0.19	0.12	0.11
GC25	0.16	-0.10	-0.15	0.03
GC27	0.31	0.03	0.18	-0.04
GC28	-0.10	0.14	0.05	0.27
GC29	0.10	0.09	0.00	0.26
GC37	-0.04	0.13	0.18	0.30
GC44	0.29	0.03	-0.12	0.12
α Boo	-0.53	0.37 ^a	0.33	0.11 ^a
BD-012971	-0.78	0.32	0.29	0.28
HD 142173	-0.77	0.28	0.28	0.16
HD 171877	-0.93	0.47	0.46	0.38
HD 225245	-1.16	0.46	0.36	0.26
HD 313132	-0.20	0.32	0.30	0.27
HD 343555	-0.74	0.45	0.45	0.42
HD 787	-0.16	0.15	0.09	0.15

Notes.^a Mg and Ca abundances from Ramírez & Allende Prieto (2011).

Table 3. Uncertainties in the derived abundances due to typical variations (or uncertainties) in the stellar parameters for a typical star with $T_{\text{eff}} = 3700$ K, $\log g = 1.5$, $\xi_{\text{micro}} = 2.0$ km s⁻¹, and solar metallicity.

Uncertainty	$\delta[\text{Fe}/\text{H}]$	$\delta[\text{Mg}/\text{Fe}]$	$\delta[\text{Si}/\text{Fe}]$	$\delta[\text{Ca}/\text{Fe}]$
$\delta T_{\text{eff}} = +150$ K	+0.02	-0.02	-0.10	+0.07
$\delta \log g = +0.5$	+0.02	-0.02	± 0.00	-0.01
$\delta[\text{Fe}/\text{H}] = +0.1$		-0.08	-0.09	-0.08
$\delta \xi_{\text{micro}} = +0.5$	-0.10	-0.07	-0.03	+0.06

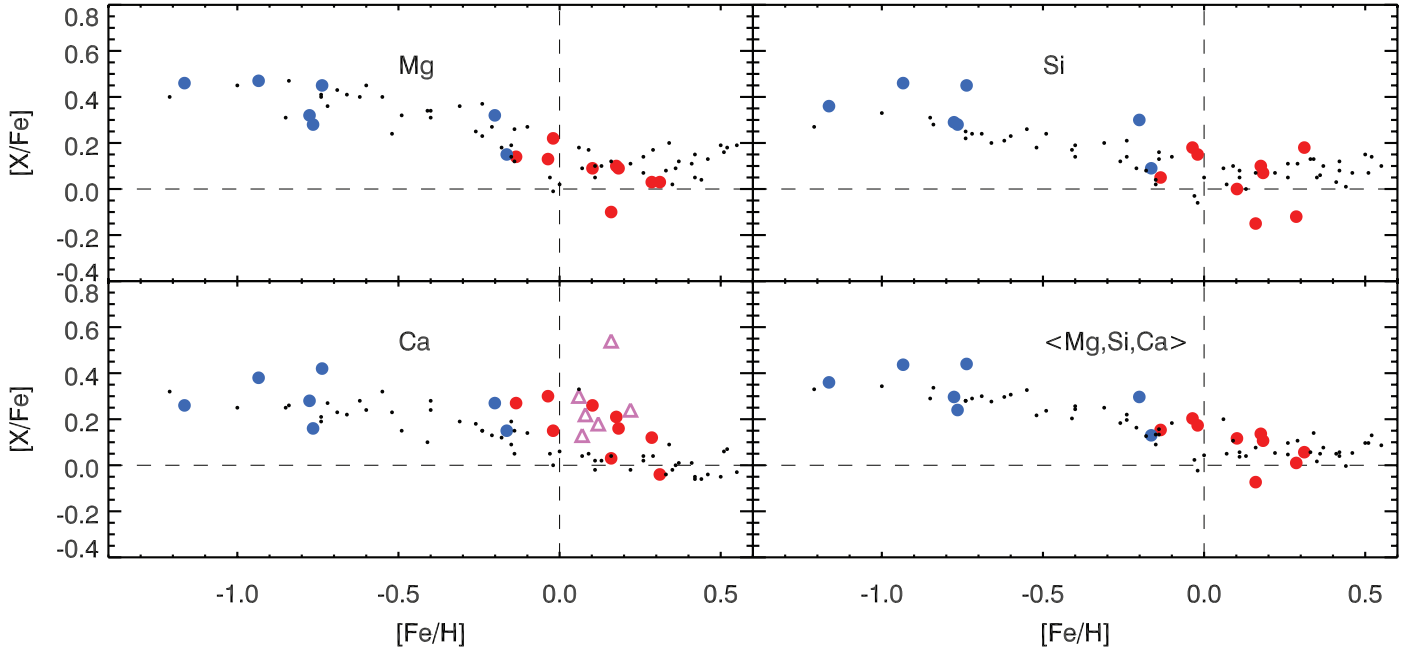


Fig. 5. Abundances trends of $[Mg/Fe]$, $[Si/Fe]$, and $[Ca/Fe]$, as well as the mean of these. Red dots mark our Galactic Centre stars, blue dots our local disk star measurements, and magenta triangles mark the $[Ca/Fe]$ measurements (with uncertainties of ± 0.15 dex) of M giants (with $M_{bol} > -5.5$) in the GC by Cunha et al. (2007). The black small dots are the abundances determinations based on micro-lensed dwarfs by Bensby et al. (2013).

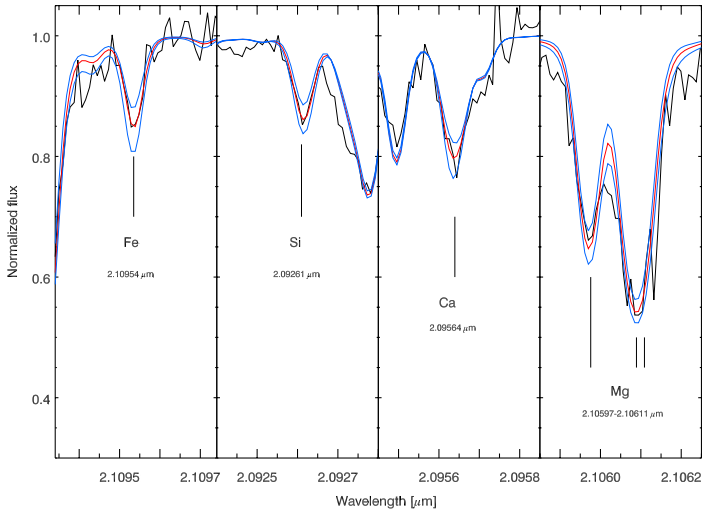


Fig. 4. Sensitivity of typical spectral lines for a change of the abundance of Fe, Si, Ca, and Mg, respectively. The red spectrum shows the best fit and the blue ones show the spectra for a change of ± 0.2 dex in abundance. The star in this case is GC28.

tematic uncertainties could be important. In order to reduce random and systematic uncertainties, we therefore also plot a mean of the three trends in the lower right panel. From this plot it is evident that we can not claim that our $[\alpha/Fe]$ trend in the GC is particular compared to the outer bulge. However, more investigations on the $[Ca/Fe]$ trend is needed to verify its high trend in the GC.

Figure 6 shows the tight metallicity distribution with $[Fe/H] = +0.11 \pm 0.15$ and the total spread in metallicities of 0.41 dex. Our mean metallicity distribution is close to that found by Cunha et al. (2007), indicated by the red histogram. However, our total spread is broader than theirs of 0.16, but it is much smaller than found typical for giants in the Galac-

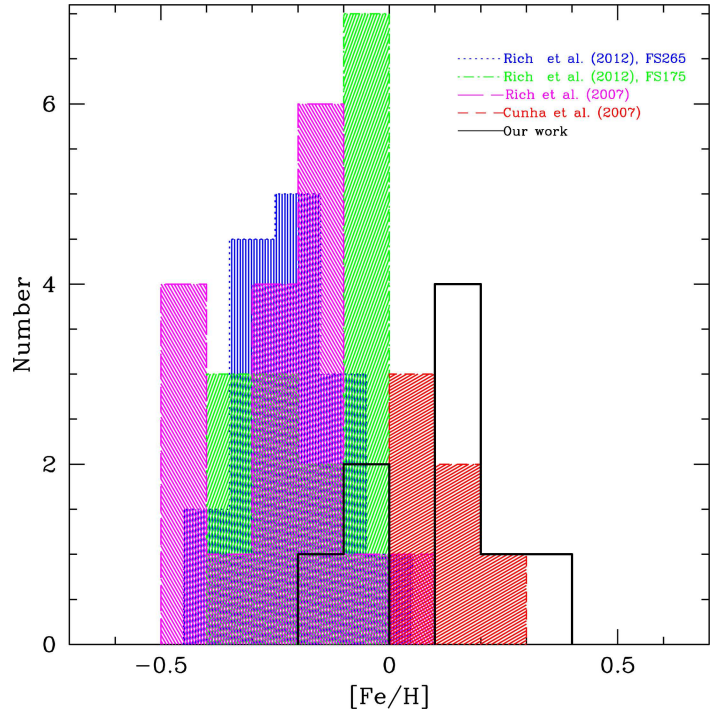


Fig. 6. Histogram of our metallicities in black with a mean of $[Fe/H]=0.11$ and a standard deviation of 0.15. The red histogram shows the metallicities of the Galactic centre giants of Cunha et al. (2007). For comparison we show in magenta the field of Rich et al. (2007) located at $(l,b)=(0^\circ, -1^\circ)$, in green the field at $(0^\circ, -1.75^\circ)$ (Rich et al. 2012) and in blue the field at $(1^\circ, -2.65^\circ)$ (Rich et al. 2012).

tic Bulge (see e.g. the metallicity distributions of Zoccali et al. (2003), Fulbright et al. (2006), Hill et al. (2011)), and Ness et al. (2013). The most striking feature is clearly the absence of the metal-poor population with no stars below -0.1 dex in $[Fe/H]$ in

agreement with the work of Cunha et al. (2007). This strengthens the argument of a specific population different to those of the Bulge. Fields in the inner Bulge located at $b = -1^\circ$ (Rich et al. 2007) (magenta) and $b = -1.65^\circ$ (green) as well as $b = -2.65^\circ$ (blue) (Rich et al. 2012) have mean metallicities at $[\text{Fe}/\text{H}] = -0.22$, $[\text{Fe}/\text{H}] = -0.16$, and $[\text{Fe}/\text{H}] = -0.21$, which are ~ 0.3 dex lower than our metallicities in the GC (see Fig. 6).

In Figure 7 we show our abundance-ratio trends again, but now together with those of the inner Bulge fields, as derived by Rich et al. (2007) and Rich et al. (2012), shifted to the solar scale of Grevesse et al. (2007), which we use in our analysis. It is clear again that our metallicities are generally higher, with a small overlap. Although there are certainly systematic uncertainties that could make a comparison difficult, it is worth discussing; Compared to the large difference in the metallicities of the stars, the $[\alpha/\text{Fe}]$ abundance ratios agree quite well, although our values tend to be of the order of 0.1 dex lower. It is interesting to note that the $[\text{Ca}/\text{Fe}]$ versus $[\text{Fe}/\text{H}]$ trend seem to show higher values from all the inner fields compared to the micro-lensed dwarf sample.

In Figure 7 we also plot the mean abundances of the two populations in the complex globular cluster Terzan 5 located in the inner Bulge, $(l, b) = (3.8^\circ, +1.7^\circ)$, as derived by Origlia et al. (2011) (in green squares in Figure 7). It is interesting that the metal-rich population at $[\text{Fe}/\text{H}] = +0.27$, shows solar $[\alpha/\text{Fe}]$, similar to our GC population at that metallicity. However, in contrast to Terzan 5, we clearly miss a distinct metal-poor population. Origlia et al. (2011) suggest that there might be a common origin and evolution of field populations in the Bulge and Terzan 5, the latter perhaps being a relic building block of the Bulge.

Thus, we see a metal-rich but low α -enhanced population in the GC. This finding would rule out a scenario that SNIIE played the dominated role in the chemical enrichment of the gas associated with a rapid formation. Again we find a significant difference compared to the high α -enhanced values of Rich et al. (2007, 2012) indicating that the GC population is different. The metal-rich population of Terzan 5 shows similarities to our GC population.

The presence of a double bar in our Galaxy which can be observed in external galaxies (Laine et al. 2002; Erwin 2004) is still questioned. Alard (2001), Nishiyama et al. (2005), and Gonzalez et al. (2011) claim that there is an inner structure distinct to the large-scale Galactic bar, with a different orientation angle which could be associated with a secondary, inner bar. On the other hand, Gerhard & Martinez-Valpuesta (2012) can explain this inner structure by dynamical instabilities from the disk without requiring a nuclear bar. The metal-rich metallicities together with low α -enhancement that we derive for the GC stars in our study presented here, seems to indicate a bar-like population (as seen by Babusiaux et al. (2010) for the main bar) most likely related to the nuclear bar.

Detailed chemical evolution models for the central 200 pc of the GC, taking into account the increased star formation history, star formation efficiency, various gas-infall and gas outflow mechanisms, including the possible role of the nuclear bar are unfortunately missing. Detailed chemical/dynamical modelling of this extreme part of our Galaxy is needed for a proper interpretation of the observables but also for Bulge formation models in general.

Acknowledgements. The anonymous referee is thanked for suggestions that improved the paper. Nils Ryde is a Royal Swedish Academy of Sciences Research Fellow supported by a grant from the Knut and Alice Wallenberg Foundation, and acknowledges support from the Swedish Research Council, VR (project number 621-2008-4245), Funds from Kungl. Fysiografiska Sällskapet i Lund.

(Stiftelsen Walter Gyllenbergs fond and Märta och Erik Holmbergs donation). This publication makes use of data products from the Two Micron All Sky Survey, which is a joint project of the University of Massachusetts and the Infrared Processing and Analysis Center/California Institute of Technology, funded by the National Aeronautics and Space Administration and the National Science Foundation. This work has made use of the VALD database, operated at Uppsala University, the Institute of Astronomy RAS in Moscow, and the University of Vienna.

References

- Alard, C. 2001, *A&A*, 379, L44
 Babusiaux, C., Gómez, A., Hill, V., et al. 2010, *A&A*, 519, A77
 Bensby, T., Yee, J. C., Feltzing, S., et al. 2013, *A&A*, 549, A147
 Blum, R. D., Ramírez, S. V., Sellgren, K., & Olsen, K. 2003, *ApJ*, 597, 323
 Cardelli, J. A., Clayton, G. C., & Mathis, J. S. 1989, *ApJ*, 345, 245
 Carr, J. S., Sellgren, K., & Balachandran, S. C. 2000, *ApJ*, 530, 307
 Cunha, K., Sellgren, K., Smith, V. V., et al. 2007, *ApJ*, 669, 1011
 Davies, B., Origlia, L., Kudritzki, R.-P., et al. 2009, *ApJ*, 694, 46
 Erwin, P. 2004, *A&A*, 415, 941
 Fulbright, J. P., McWilliam, A., & Rich, R. M. 2006, *ApJ*, 636, 821
 Gerhard, O. & Martinez-Valpuesta, I. 2012, *ApJ*, 744, L8
 Girard, T. M., Dinescu, D. I., van Altena, W. F., et al. 2004, *AJ*, 127, 3060
 Gonzalez, O. A., Rejkuba, M., Zoccali, M., et al. 2011, *A&A*, 530, A54
 Grevesse, N., Asplund, M., & Sauval, A. J. 2007, *Space Sci. Rev.*, 130, 105
 Grieco, V., Matteucci, F., Pipino, A., & Cescutti, G. 2012, *A&A*, 548, A60
 Gustafsson, B., Edvardsson, B., Eriksson, K., et al. 2008, *A&A*, 486, 951
 Hill, V., Lecœur, A., Gómez, A., et al. 2011, *A&A*, 534, A80
 Hinkle, K., Wallace, L., & Livingston, W. C. 1995, *Infrared atlas of the Arcturus spectrum, 0.9-5.3 microns* (San Francisco, Calif.: Astronomical Society of the Pacific, 1995.)
 Houdashelt, M. L., Bell, R. A., & Sweigart, A. V. 2000, *AJ*, 119, 1448
 Ivanov, V. D., Rieke, M. J., Engelbracht, C. W., et al. 2004, *ApJS*, 151, 387
 Jørgensen, U. G. & Larsson, M. 1990, *A&A*, 238, 424
 Käufel, H.-U., Ballester, P., Biereichel, P., et al. 2004, in Presented at the Society of Photo-Optical Instrumentation Engineers (SPIE) Conference, Vol. 5492, Society of Photo-Optical Instrumentation Engineers (SPIE) Conference Series, ed. A. F. M. Moorwood & M. Iye, 1218–1227
 Klein Gebbink, M., & Sforna, D. 2007, *VERY LARGE TELESCOPE: Gasgano User's Manual*
 Laine, S., Shlosman, I., Knapen, J. H., & Peletier, R. F. 2002, *ApJ*, 567, 97
 Lawrence, A., Warren, S. J., Almaini, O., et al. 2013, *VizieR Online Data Catalog*, 2319, 0
 Livingston, W. & Wallace, L. 1991, *An atlas of the solar spectrum in the infrared from 1850 to 9000 cm⁻¹ (1.1 to 5.4 micrometer)* (NSO Technical Report, Tucson: National Solar Observatory, National Optical Astronomy Observatory, 1991)
 Matteucci, F. 2012, *Chemical Evolution of Galaxies*
 Minniti, D., Lucas, P. W., Emerson, J. P., et al. 2010, *New A*, 15, 433
 Monaco, L., Villanova, S., Moni Bidin, C., et al. 2011, *A&A*, 529, A90
 Moorwood, A., Cuby, J.-G., Biereichel, P., et al. 1998, *The Messenger*, 94, 7
 Najaro, F., Figer, D. F., Hillier, D. J., Geballe, T. R., & Kudritzki, R. P. 2009, *ApJ*, 691, 1816
 Ness, M., Freeman, K., Athanassoula, E., et al. 2013, *MNRAS*, 430, 836
 Nishiyama, S., Nagata, T., Baba, D., et al. 2005, *ApJ*, 621, L105
 Nishiyama, S., Tamura, M., Hatano, H., et al. 2009, *ApJ*, 696, 1407
 Origlia, L., Rich, R. M., & Castro, S. 2002, *AJ*, 123, 1559
 Origlia, L., Rich, R. M., Ferraro, F. R., et al. 2011, *ApJ*, 726, L20
 Piskunov, N. E., Kupka, F., Ryabchikova, T. A., Weiss, W. W., & Jeffery, C. S. 1995, *A&AS*, 112, 525
 Ramírez, I. & Allende Prieto, C. 2011, *ApJ*, 743, 135
 Ramirez, S. V., Depoy, D. L., Frogel, J. A., Sellgren, K., & Blum, R. D. 1997, *AJ*, 113, 1411
 Ramírez, S. V., Sellgren, K., Carr, J. S., et al. 2000, *ApJ*, 537, 205
 Rich, R. M. & Origlia, L. 2005, *ApJ*, 634, 1293
 Rich, R. M., Origlia, L., & Valenti, E. 2007, *ApJ*, 665, L119
 Rich, R. M., Origlia, L., & Valenti, E. 2012, *ApJ*, 746, 59
 Schultheis, M., Chen, B. Q., Jiang, B. W., et al. 2014, *ArXiv e-prints*
 Schultheis, M., Sellgren, K., Ramírez, S., et al. 2009, *A&A*, 495, 157
 Silk, J. & Wyse, R. F. G. 1993, *Phys. Rep.*, 231, 293
 Smoker, J. 2007, *Very Large Telescope Paranal Science Operations CRIRES User Manual*
 Smoker, J., Valenti, E., Asmus, D., et al. 2012, *Very Large Telescope Paranal Science Operations CRIRES data reduction cookbook*
 Tody, D. 1993, in *ASP Conf. Ser. 52: Astronomical Data Analysis Software and Systems II*, ed. R. J. Hanisch, R. J. V. Brissenden, & J. Barnes, 173
 Tsuji, T. 2008, *A&A*, 489, 1271
 Valenti, J. A. & Piskunov, N. 1996, *A&AS*, 118, 595
 Valenti, J. A. & Piskunov, N. 2012, *SME: Spectroscopy Made Easy*, astrophysics Source Code Library
 Zoccali, M., Hill, V., Lecœur, A., et al. 2008, *A&A*, 486, 177
 Zoccali, M., Renzini, A., Ortolani, S., et al. 2003, *A&A*, 399, 931

Article number, page 7 of 8

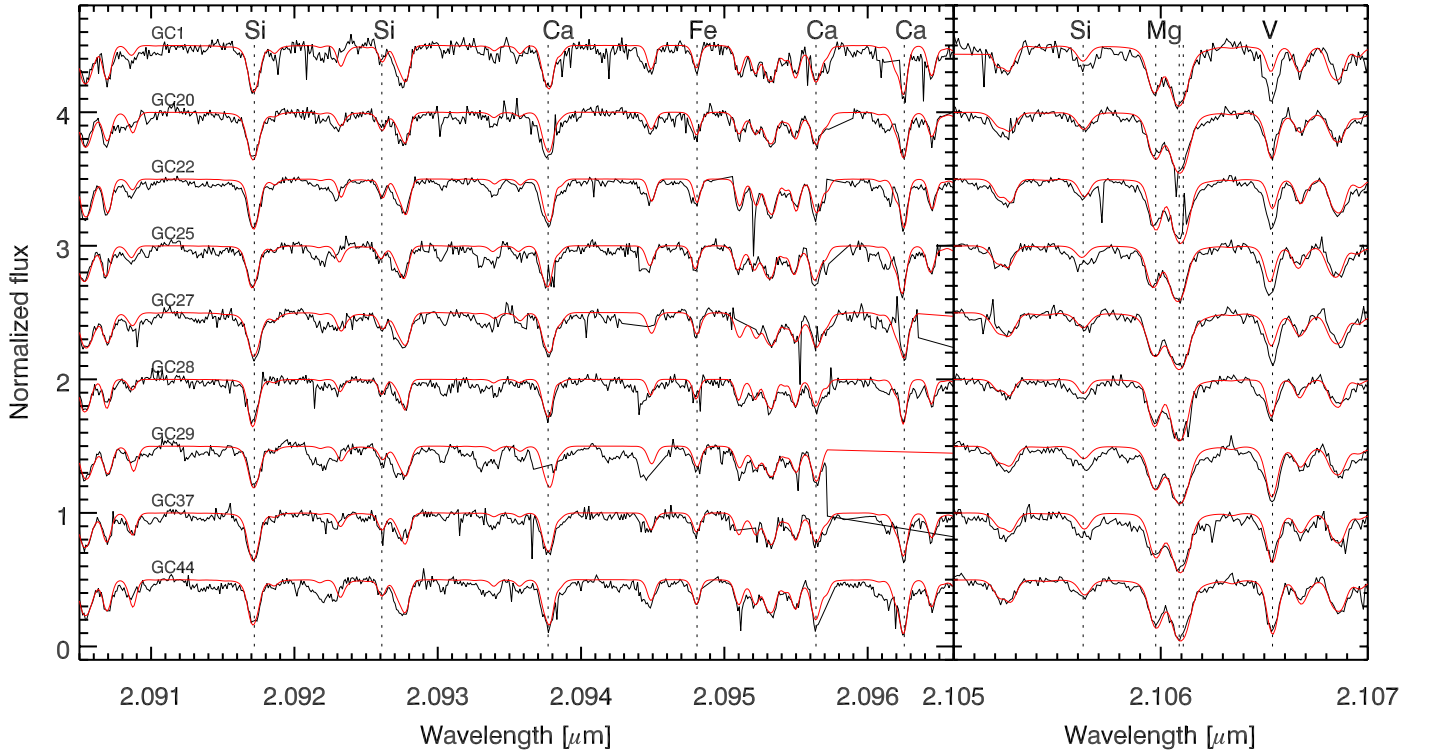


Fig. 8. Observed spectra of all our Galactic Centre stars are shown in black. The best synthetic spectra are shown in red.

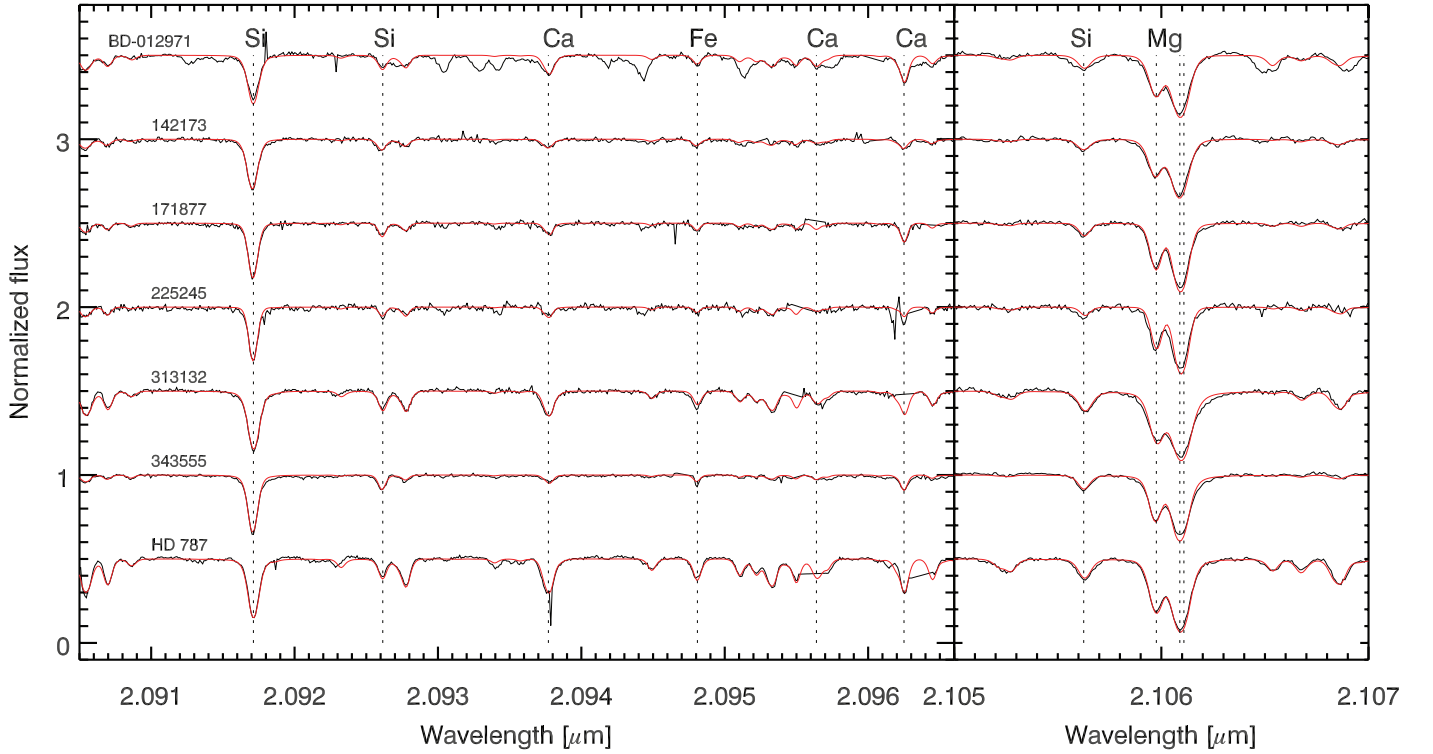


Fig. 9. Observed spectra of all our Galactic Centre stars are shown in black. The best synthetic spectra are shown in red.